

EFFECTS OF MEMBRANE POTENTIAL AND MUSCARINE ON POTASSIUM M-CHANNEL KINETICS IN RAT SYMPATHETIC NEURONES

BY A. A. SELYANKO AND D. A. BROWN

From the Department of Pharmacology, University College London, Gower Street, London WC1E 6BT

(Received 18 February 1993)

SUMMARY

1. Using cell-attached patch pipettes, sustained activity of single potassium M-channels was recorded from dissociated rat superior cervical ganglion neurones. Previous results indicated that this activity, consisting of three main levels of open-channel conductance (≈ 7 , ≈ 12 and ≈ 19 pS) was activated by membrane depolarization and inhibited by muscarine added outside the patch. Consequently, a kinetic analysis was undertaken in order to identify M-channel states sensitive to muscarine and membrane potential.

2. Channel activity recorded at 30 mV positive to the resting membrane potential level (≈ -60 mV) showed three shut and two open times. Mean shut times were: $\tau_{s1} = 8.0 \pm 2.2$ ms; $\tau_{s2} = 71.3 \pm 8.6$ ms and $\tau_{s3} = 740 \pm 220$ ms. Mean open times were: $\tau_{o1} = 10.6 \pm 1.9$ ms and $\tau_{o2} = 59.3 \pm 8.7$ ms. When bursts of channel openings were determined as those including τ_{s1} , two exponential components were evident in burst duration distributions ($\tau_{b1} = 11.0 \pm 0.9$ ms and $\tau_{b2} = 80.4 \pm 11.0$ ms).

3. Membrane hyperpolarization significantly lengthened all three shut times and shortened both open times. It also slightly enhanced the relative contribution of high-conductance channels and decreased the relative contribution of low-conductance channels to overall activity.

4. All three shut times of the M-channels were lengthened by 10 μ M muscarine without significantly affecting their open times.

5. It is concluded that both open and shut states of the M-channel are voltage sensitive while only shut states are sensitive to muscarine.

INTRODUCTION

The M-current ($I_{K(M)}$) is a non-inactivating, time-dependent potassium current which is activated at membrane potentials (V_m) positive to the resting level and inhibited by muscarinic receptor stimulants (Brown & Adams, 1980). Synaptic inhibition of $I_{K(M)}$ underlies slow transmission in various types of autonomic and central neurones (for reviews see Brown, 1983, 1988*a, b*). Initial observations made on amphibian sympathetic neurones indicated that $I_{K(M)}$ activation and deactivation follow a single-exponential time course and that the time constant of $I_{K(M)}$ relaxation

(τ_M) is maximal at about -35 mV membrane potential, decreasing when the membrane was either hyper- or depolarized from this level (Adams, Brown & Constanti, 1982a). It was proposed that the M-channel has only one open and one shut state and that the rates of M-channel opening and closing are increased and decreased, respectively, with membrane depolarization (Adams *et al.* 1982a).

Although this scheme was generally confirmed by studies of $I_{K(M)}$ in a variety of nerve cells and cell lines (see Brown, 1988a, b), some evidence suggests that it may be an oversimplification. Firstly, two or three kinetic components were detected in noise spectra and relaxations associated with $I_{K(M)}$ recorded from rat (Owen, Marsh & Brown, 1990) and frog (Marrion, Adams & Gruner, 1992) sympathetic neurones, and from rodent neuroblastoma \times glioma hybrid cells (Neher, Marty, Fukuda, Kubo & Numa, 1988; Robbins, Trouslard, Marsh & Brown, 1992), suggesting there may be at least four different kinetic states of the M-channel. Secondly, some 'saturation' in the τ_M - V_m relationship was noted at strongly depolarized membrane potentials (Pennefather, 1986). Thirdly, multiple open and shut times were deduced from single-channel recordings in outside-out patches from dissociated rat ganglion cells (Stansfeld, Marsh, Gibb & Brown, 1993). However, the voltage dependence of these kinetic parameters was not determined.

In contrast to membrane potential, muscarinic acetylcholine receptor stimulation (Brown & Adams, 1980; Constanti & Brown, 1981; Adams, Brown & Constanti, 1982b; Brown, Marrion & Smart, 1989; Marrion *et al.* 1992) or a subsequent step, G-protein activation (Pfaffinger, 1988; Lopez & Adams, 1989; Brown *et al.* 1989), modulates $I_{K(M)}$ amplitude without affecting the relaxation kinetics of the macroscopic current. It was therefore suggested that these factors reduce the availability of the M-channels, without affecting their gating. However, this suggestion has not been verified directly by single-channel recording.

Single-channel activity underlying the M-current has been identified in excised (Stansfeld, Marsh & Brown, 1990; Stansfeld *et al.* 1993) and cell-attached (Selyanko, Stansfeld & Brown, 1992) patches from rat superior cervical ganglion neurones. In cell-attached patches, in accord with the properties of $I_{K(M)}$, activity persisted for many minutes, was facilitated by membrane depolarization and was inhibited by muscarine; muscarine was found to be effective only when applied to the membrane outside the patch, implying that a diffusible second messenger is necessary to close M-channels (Selyanko *et al.* 1992). In the present work the behaviour of these single channels has been further analysed in order to determine the kinetic states of the M-channel and their dependence on membrane potential and muscarinic acetylcholine receptor activation.

METHODS

Experiments were performed on superior cervical sympathetic neurones from 17-day-old rats in dissociated cell culture (Marrion, Smart & Brown, 1987; Owen *et al.* 1990). Methods of cell-attached recording of M-channel activity and its computer analysis have been described elsewhere (Selyanko *et al.* 1992).

When recorded from cell-attached patches, M-channels exhibit openings to three different levels of conductance, about 7, 12 and 19 pS (Selyanko *et al.* 1992). Channel open and shut states were identified on the basis of crossing the 50% level of the smallest channel amplitude. Currents were filtered at 250 Hz (-3 dB Bessel filter) and digitized at 2 kHz. Events shorter than 2 ms were ignored. Because the event threshold was set at half of the smallest channel amplitude, one could

expect the duration of larger channels to be somewhat overestimated. However, this effect was calculated to be negligibly small. Patches which had a small number of double channel openings were selected for the analysis. When detected these openings were discarded. A list of events was created using the PAT software provided by J. Dempster (University of Strathclyde, UK) and analysis of open and shut times was performed using software created by D. Colquhoun and A. Gibb (University College, London).

The effect of membrane potential on M-channel activity was studied in cells perfused with normal saline solution (mM: 144 NaCl, 2.5 KCl, 2 CaCl₂, 0.5 MgCl₂, 5 Hepes, 10 glucose, pH 7.4), whereas the effect of muscarine was studied on cells bathed in a modified solution having elevated [K⁺] (25 mM) and [Mg²⁺] (7 mM) with no Ca²⁺, to prevent voltage responses to muscarine and calcium loading at the depolarized membrane potential. In both types of experiment cell-attached pipettes were filled with the normal external solution. Data are expressed as means \pm s.e.m. Zero patch potential corresponds to the resting membrane potential of about -60 mV in normal solution and about -30 mV in modified solution (see Selyanko *et al.* 1992).

RESULTS

Identification of open and closed states

Figure 1A shows examples of M-channel currents, recorded from the same patch, which had three different amplitudes. Their mean values (0.25, 0.45 and 0.67 pA) were determined by fitting the open-point amplitude histogram with three Gaussian curves (Fig. 1B). Although the threshold for detecting events was set at the level corresponding to 50% of the low-amplitude current, it can be seen that channel transitions between closed and each of the open states can be fully resolved (Fig. 1A).

Effect of membrane potential

Kinetic analysis was undertaken with ten patches held for at least 2 min at each of four patch pipette potentials, -10 , -20 , -30 and -40 mV (i.e. at membrane potentials 10, 20, 30 and 40 mV depolarized relative to rest). Channels showed sustained activity at each potential, which increased markedly with increasing patch depolarization (Fig. 2A). Between 10 and 30 mV depolarization, open probability (P_o) increased e-fold for about 8 mV depolarization, with a maximum slope factor of about 6.5 mV at low P_o (Fig. 2B).

Low- and medium-conductance channels were present in all ten patches, whereas high-conductance channels were identified in eight patches only. Mean conductances were 7.0 ± 0.6 , 11.5 ± 1.0 and 17.2 ± 2.0 pS for low-, medium- and high-conductance channels respectively. The activity of low-conductance channels predominated in seven patches whereas medium-conductance channels predominated in the other three patches. Each conductance component initially present at 10 mV depolarization persisted at all membrane potentials tested. However, the contribution of high-conductance channels increased with membrane depolarization ($P < 0.05$), whereas that of low-conductance channels decreased (Fig. 2C).

Three shut and two open times were identified in M-channel activity recorded in the range of -10 to -40 mV pipette potential (Figs 3 and 4 and Table 1). There was no obvious dependence of kinetic parameters on the presence or absence of high-conductance channels or the dominance of low- or medium-conductance channels in the patch. The shut times were reduced and the open times were increased by membrane depolarization; these changes were most pronounced for the slowest shut

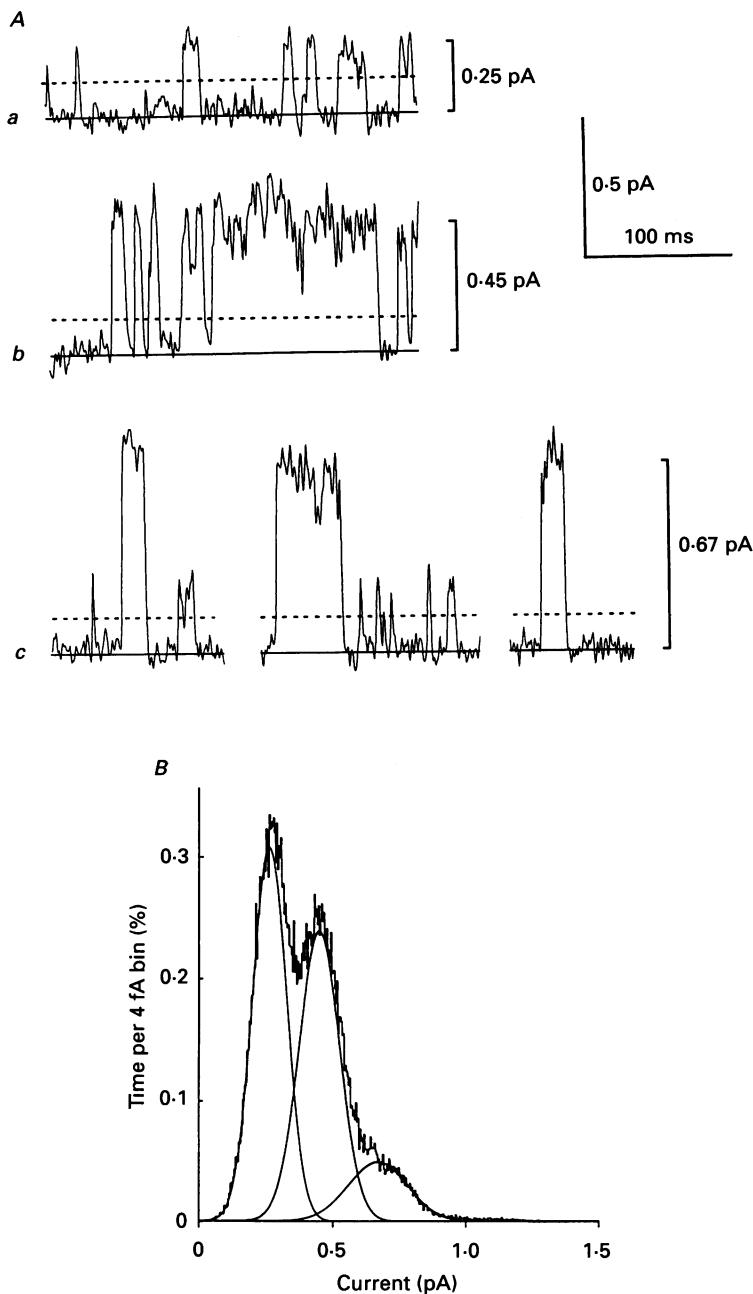


Fig. 1. Detection of events in M-channel activity. *A*, examples of currents produced by low-conductance (*a*), medium-conductance (*b*) and high-conductance (*c*) M-channels and identification of channel open and shut states on the basis of crossing the 50% level (interrupted line) of the smallest channel amplitude. Continuous horizontal lines denote zero current level. Vertical bars show current amplitudes for low-conductance (0.25 pA), medium-conductance (0.45 pA) and high-conductance (0.67 pA) channels estimated from a three-component open-point histogram. All records were obtained from the same patch with normal (2.5 mM K⁺) solution both in the pipette and in the perfusion solution.

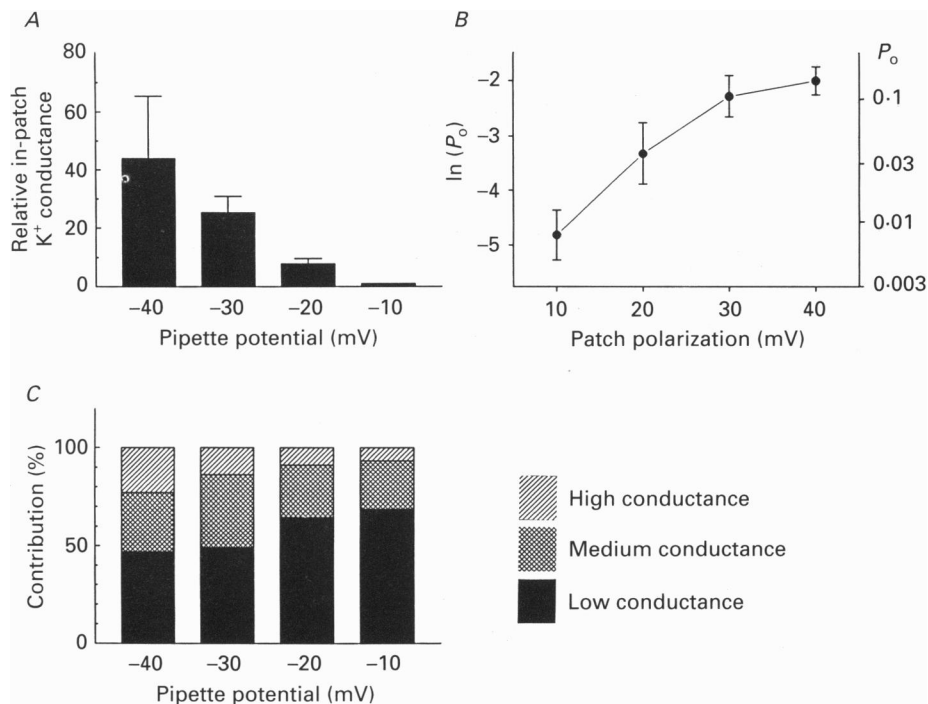


Fig. 2. Voltage dependence of M-channel activity. *A*, mean in-patch conductance (estimated as charge transfer per unit time divided by the electrical driving force, see Selyanko *et al.* 1992) plotted against pipette potential. Conductances at each potential were normalized to those at -10 mV pipette potential ($= 1$). Vertical bars show s.e.m. ($n = 10$). *B*, plot of $\ln(P_o)$ against membrane depolarization, determined from open-point histograms for all channel openings over 2 min. Each point is the mean of 10 patches; bars show s.e.m. *C*, relative contributions of channels with different conductances (see Fig. 1) to the overall conductance recorded at each pipette potential. Overall P_o at each potential is taken as 100%. Blocks show contributions of channels with highest conductance (top bar, hatched), medium conductance (middle bar, cross-hatched) and lowest conductance (lowest block, filled).

and open states. Thus, it is probably the voltage dependence of channel kinetics which accounts for the increase in patch M-conductance shown above (Fig. 2).

The multi-component distribution of the shut times suggests that the M-channel openings appeared in bursts. Assuming that the burst included gaps underlying the shortest shut time component, τ_{s1} , the mean burst duration was determined using a critical shut time (t_c) calculated as in Colquhoun & Sakmann (1985). Two burst durations were detected in each patch studied. Their mean values were 11.0 ± 0.9 ms for τ_{b1} and 80.4 ± 11.0 ms for τ_{b2} at a V_m depolarized 30 mV relative to the resting level (relative contributions: 64.8 and 35.2%, respectively; $t_c = 11.2 \pm 1.2$ ms).

Pipette potential, -30 mV. *B*, open-point amplitude histogram obtained from the activity (1 min) whose fragments are shown in *A*. Current components identified by fitting the histogram with three Gaussian curves were of 0.25, 0.45 and 0.67 pA (s.d.s 0.063, 0.076 and 0.111 pA, respectively). Their relative contributions were 45.1, 42.2 and 12.7%.

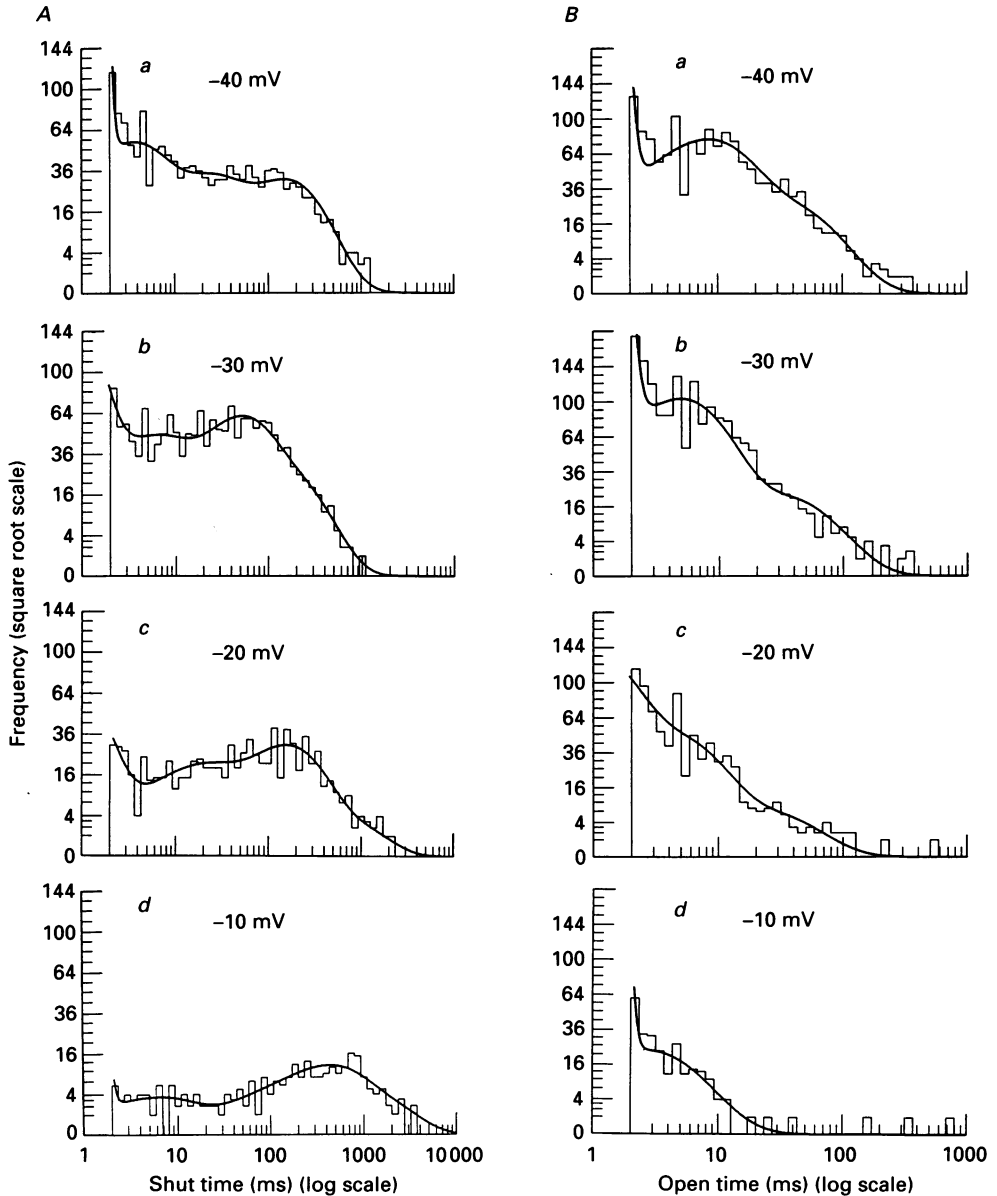


Fig. 3. Voltage dependence of the kinetics of M-channel. Shut (*A*) and open (*B*) time histograms are shown, for the activity recorded from the same patch at pipette potentials of -40 (*a*), -30 (*b*), -20 (*c*) and -10 mV (*d*). Histograms were fitted with exponential components: *Aa*, $\tau_{s1} = 3.0$ ms (43%), $\tau_{s2} = 17.2$ ms (25%) and $\tau_{s3} = 152$ ms (32%); *Ab*, $\tau_{s1} = 4.2$ ms (31%), $\tau_{s2} = 41.6$ ms (44%) and $\tau_{s3} = 144$ ms (25%); *Ac*, $\tau_{s1} = 13.3$ ms (29%), $\tau_{s2} = 147$ ms (63%) and $\tau_{s3} = 501$ ms (8%); *Ad*, $\tau_{s1} = 5.5$ ms (19%), $\tau_{s2} = 372$ ms (59%) and $\tau_{s3} = 1015$ ms (22%); *Ba*, $\tau_{o1} = 7.2$ ms (71%) and $\tau_{o2} = 31.9$ ms (29%); *Bb*, $\tau_{o1} = 4.6$ ms (82%) and $\tau_{o2} = 30.0$ ms (18%); *Bc*, $\tau_{o1} = 3.9$ ms (86%) and $\tau_{o2} = 19.2$ ms (14%); *Bd*, $\tau_{o1} = 2.5$ ms (91%) and $\tau_{o2} = 3.9$ ms (9%). Each histogram contained a fast, unresolved component whose contribution was ignored. The activity contained two channel conductances: 7.0 and 13.8 pS (contributions 71 and 29%, respectively).

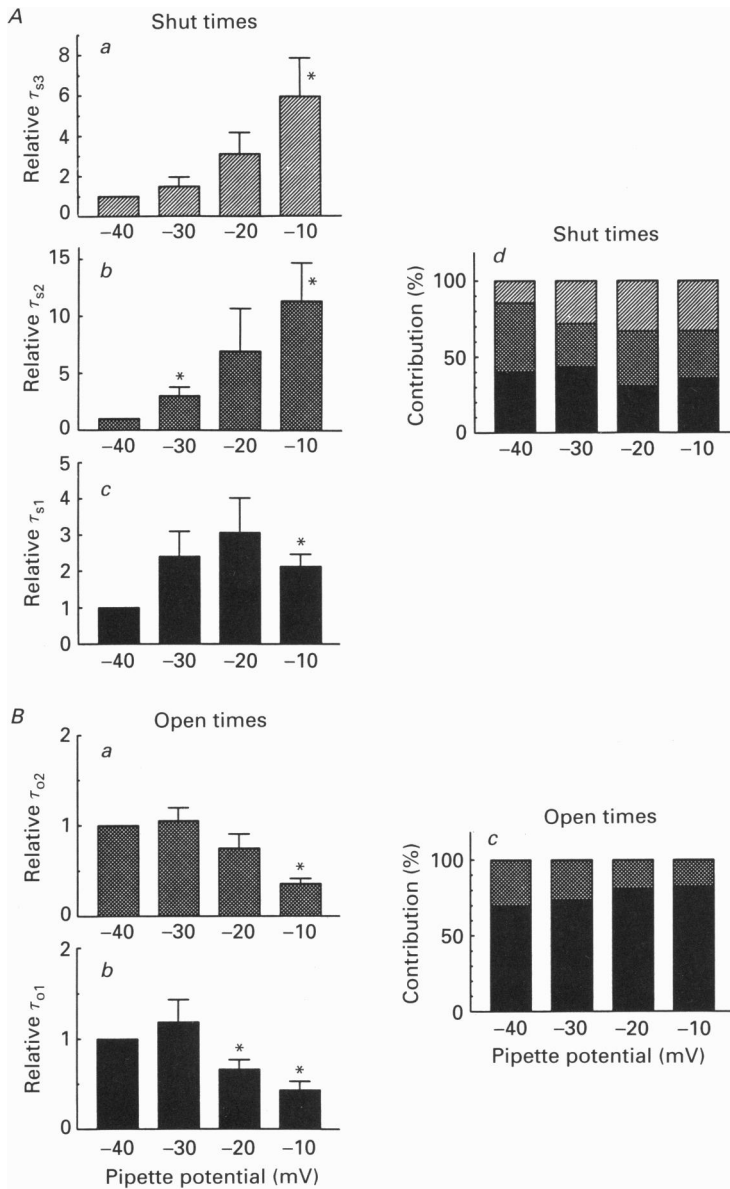


Fig. 4. Voltage dependence of kinetic components. Mean values of shut (*Aa–Ac*) and open (*Ba–Bb*) times, as well as their contributions (*Ad* and *Bc*) are plotted against pipette potential. In each patch kinetic components at -40 mV were taken as 1. Vertical lines are s.e.m.s. The data obtained from 10 patches are shown. * $P < 0.05$ compared to kinetic components at -40 mV (paired Student's *t* test).

Because the threshold for channel opening was set at 50% of the smallest current level (see Methods), the changes in apparent open and shut times shown in Fig. 4 and Table 1 might have been (in part) due to the increased current amplitudes. To check

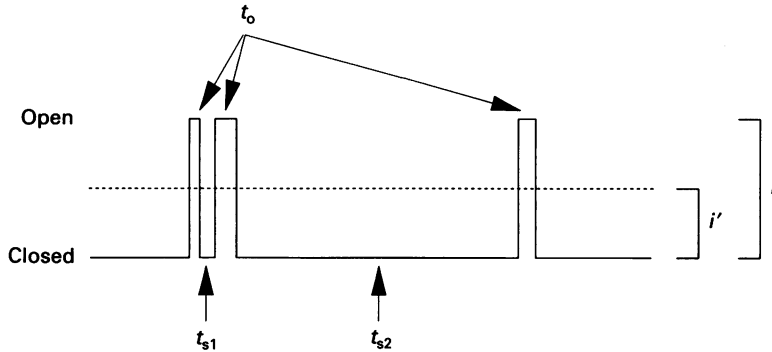


Fig. 5. Schematic representation of simulated M-channel activity. The mean values of channel open (t_o) and shut (t_{s1} and t_{s2}) times are equal to τ_o , τ_{s1} and τ_{s2} ; i and i' are current amplitude and threshold for event detection, respectively. For further explanation see text.

TABLE 1. Effect of membrane potential on kinetic components in M-channel activity

E_p^* (mV)	τ_{o1}		τ_{o2}		τ_{s1}		τ_{s2}		τ_{s3}	
	(ms)	(%)	(ms)	(%)	(ms)	(%)	(ms)	(%)	(ms)	(%)
-40	10.4 ± 1.4	69.5 ± 4.4	62.4 ± 11.4	30.4 ± 4.4	4.2 ± 0.8	39.9 ± 5.5	35.6 ± 7.7	31.6 ± 6.7	624 ± 237	24.4 ± 7.0
-30	10.6 ± 1.9	73.9 ± 4.7	59.3 ± 8.7	26.0 ± 4.7	8.0 ± 2.2	43.6 ± 6.0	71.3 ± 8.6	27.6 ± 5.8	740 ± 220	28.2 ± 8.1
-20	5.9 ± 0.6	81.0 ± 4.5	36.1 ± 8.2	18.9 ± 4.5	8.8 ± 2.0	30.7 ± 3.4	158 ± 60.6	34.0 ± 7.6	942 ± 286	33.1 ± 10.7
-10	3.8 ± 0.7	82.5 ± 9.1	17.8 ± 4.5	17.4 ± 9.1	7.4 ± 1.5	35.5 ± 5.5	293 ± 78.1	30.2 ± 8.5	1857 ± 617	32.9 ± 9.5

* Pipette potential. Data are means ± s.e.m. ($n = 10$).

TABLE 2. Kinetic parameters of events detected in simulated M-channel activity

Initial kinetic parameters	τ_o	τ_{s1}	τ_{s2}
	7.0 ms	3.0 ms (67%)	17.0 ms (33%)
Patch depolarization of 10 mV			
$i' = 0.1$ pA	$i = 0.2$ pA	6.4 ms	3.4 ms (54%)
	$i = 0.41$ pA	8.9 ms	2.3 ms (56%)
Patch depolarization of 40 mV			
$i' = 0.23$ pA	$i = 0.46$ pA	7.4 ms	3.7 ms (56%)
	$i = 0.95$ pA	9.3 ms	2.5 ms (55%)
			21.1 ms (44%)
			16.0 ms (45%)

Initial parameters for this simulation were taken from the experiment shown in Fig. 1: s.d. of background noise = 0.041 pA; current amplitude (i) of 0.2 pA and 0.46 pA for the low-amplitude current (at 10 and 40 mV depolarized to the rest) and of 0.41 and 0.95 pA for the medium-amplitude current (at 10 and 40 mV depolarized to the rest); threshold for event detection ($i' = 0.1$ and 0.23 at these two potentials); τ_o , τ_{s1} and τ_{s2} and their contributions (in parentheses) as shown in the table. See Fig. 5 and text for further explanation.

this, we ran a partial simulation of idealized small- and medium-amplitude channels at membrane potentials depolarized 10 and 40 mV from rest, based on the experiment shown in Fig. 1 (see Fig. 5). Current amplitudes for the small channel

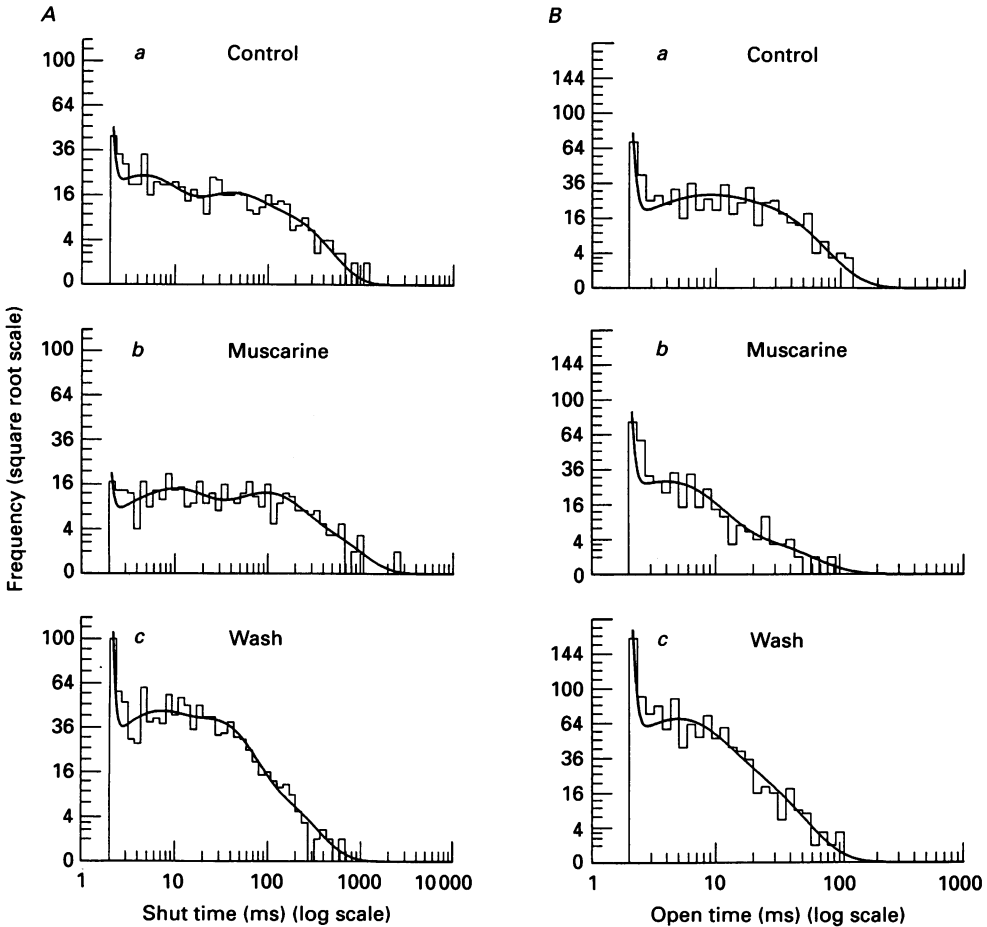


Fig. 6. Effect of muscarine on the kinetics of M-channel. Shut (*A*) and open (*B*) time histograms are shown, for the activity recorded from the same patch before (*a*), during (*b*) and after (*c*) addition of muscarine ($10 \mu\text{M}$) to the bath. Pipette potential, -10 mV . Histograms were fitted with exponential components: *Aa*, $\tau_{s1} = 3.7 \text{ ms}$ (48%), $\tau_{s2} = 29.7 \text{ ms}$ (29%) and $\tau_{s3} = 123 \text{ ms}$ (23%); *Ab*, $\tau_{s1} = 7.9 \text{ ms}$ (44%), $\tau_{s2} = 81.7 \text{ ms}$ (41%) and $\tau_{s3} = 273 \text{ ms}$ (15%); *Ac*, $\tau_{s1} = 4.3 \text{ ms}$ (39%), $\tau_{s2} = 24.2 \text{ ms}$ (49%) and $\tau_{s3} = 91.4 \text{ ms}$ (12%); *Ba*, $\tau_{o1} = 5.1 \text{ ms}$ (41%) and $\tau_{o2} = 20.1 \text{ ms}$ (59%); *Bb*, $\tau_{o1} = 3.7 \text{ ms}$ (87%) and $\tau_{o2} = 16.0 \text{ ms}$ (13%); *Bc*, $\tau_{o1} = 4.0 \text{ ms}$ (66%) and $\tau_{o2} = 14.0 \text{ ms}$ (34%). As in Fig. 3, each distribution contained a fast, unresolved component whose contribution was ignored. The activity contained a predominant conductance of 5.0 pS .

were 0.2 pA at $+10 \text{ mV}$ depolarization and 0.46 pA at $+40 \text{ mV}$; those for the larger channel were 0.41 pA at $+10 \text{ mV}$ and 0.95 pA at $+40 \text{ mV}$. At each potential the event threshold was set at half the amplitude of the small channel (i.e. 0.1 pA at $+10 \text{ mV}$ and 0.23 pA at $+40 \text{ mV}$). Random noise (s.d. 0.041 pA) was superimposed

and digitally filtered to match recorded signals. The simulation was run for one exponentially distributed open time and two exponentially distributed shut times, with means set at $\tau_o = 7$ ms, $\tau_{s1} = 3$ ms (contribution: 67%) and $\tau_{s2} = 17$ ms (contribution: 33%) (Fig. 5). The results of this simulation are given in Table 2. While there is some slight lengthening of τ_o with depolarization (and corresponding

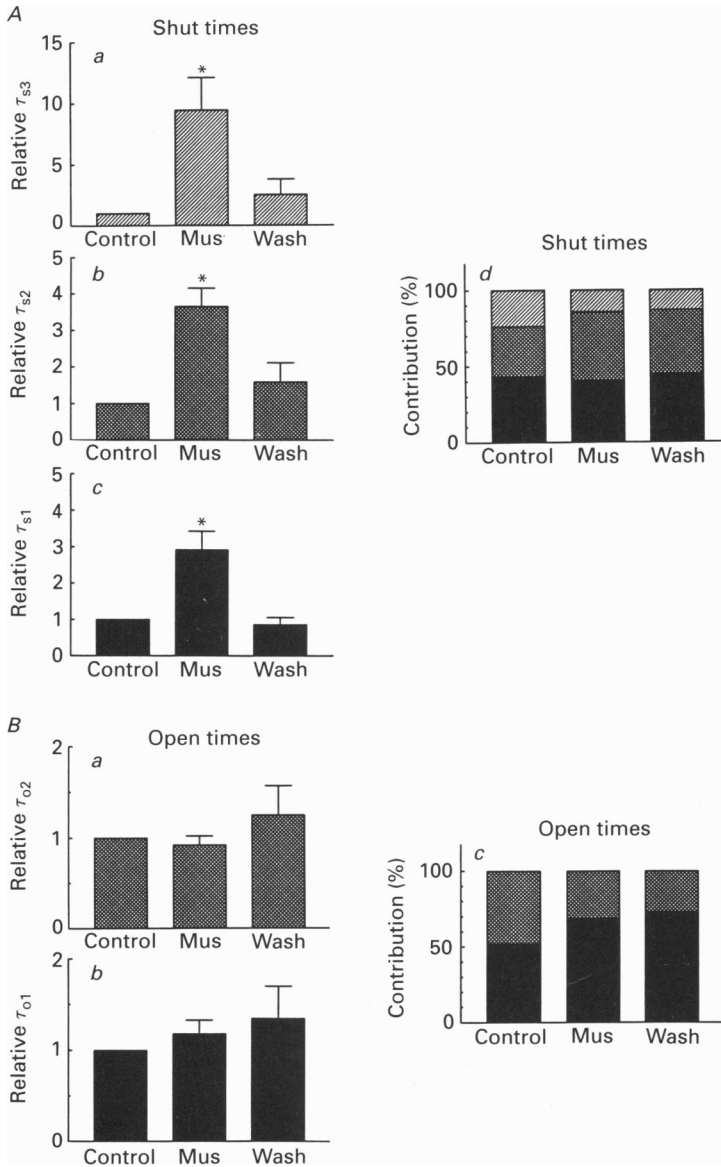


Fig. 7. Effect of muscarine on kinetic components. Mean values of shut (*Aa–Ac*) and open (*Ba–Bb*) times, as well as their contributions (*Ad* and *Bc*) are shown obtained before, during and after addition of muscarine (Mus). Vertical lines are s.e.m.s. The data obtained from 6 patches are shown. In each patch kinetic components in controls were taken as 1. * $P < 0.05$ compared to controls (paired Student's *t* test).

shortening of both shut times), these are much less than those recorded experimentally (cf. Table 1). Clearly, changes in the longer open and shut times (τ_{o2} and τ_{s3}) would be even less susceptible to distortion through changes in current amplitude.

Effect of muscarine

The effect of muscarine on M-channel activity was tested on cells bathed in a solution containing 25 mM K⁺. We have previously reported that this depolarized

TABLE 3. Effect of muscarine (10 μ M) on kinetic components in M-channel activity

	τ_{s1}		τ_{s2}			
	(ms)	(%)	(ms)	(%)		
Control	4.0 \pm 0.8	52.2 \pm 13.5	25.3 \pm 6.6	47.3 \pm 13.5		
Muscarine	4.2 \pm 0.6	68.5 \pm 8.4	22.5 \pm 9.2	30.9 \pm 8.2		
Wash	4.8 \pm 1.1	73.1 \pm 3.7	24.4 \pm 4.9	26.8 \pm 3.7		

	τ_{s1}		τ_{s2}		τ_{s3}	
	(ms)	(%)	(ms)	(%)	(ms)	(%)
Control	5.5 \pm 1.6	43.2 \pm 10.5	48.0 \pm 17.6	32.9 \pm 5.5	245 \pm 101	23.8 \pm 11.6
Muscarine	13.1 \pm 3.6	40.2 \pm 11.4	169 \pm 70.5	45.6 \pm 9.2	1456 \pm 721	14.1 \pm 4.8
Wash	3.6 \pm 0.8	44.5 \pm 11.8	59.5 \pm 35.0	42.3 \pm 8.6	298 \pm 157	13.0 \pm 3.6

Data are means \pm S.E.M. ($n = 6$).

the membrane by about 30 mV (Selyanko *et al.* 1992). The recording of M-channel activity was made at an in-patch membrane potential 0–10 mV more positive than this depolarized level. For the analysis of muscarine effect on M-channel kinetics the data obtained from six patches were selected where (i) the control activity was not obviously contaminated by current superimpositions and (ii) the effect of muscarine on channel activity was most prominent, i.e. charge transfer through the patch was reduced to 12.6 \pm 2.6% (S.E.M.; range, 6–23%) of its control level. The analysis showed that muscarine lengthened all shut times without significantly changing open times of the M-channels. (Figs 6 and 7 and Table 3). At the same time, muscarine did not clearly change the relative contributions of the different kinetic states to the overall activity. Thus, the effect of muscarine was to reduce the frequency of channel openings rather than their durations.

In this series of experiments, the burst duration components obtained at resting membrane potential in the controls ($\tau_{b1} = 11.1 \pm 2.0$ ms and $\tau_{b2} = 102 \pm 27.7$ ms; relative contributions: 53.8% and 46.2%; $t_c = 9.7 \pm 3.5$ ms) were not significantly different from corresponding components obtained at a membrane potential depolarized by 30 mV in normal bathing solution (see above).

DISCUSSION

In agreement with recent observations on isolated patches (Stansfeld *et al.* 1993), the present work shows that at least three shut and two open states can be detected

in the activity of single M-channels recorded from cell-attached patches from rat sympathetic neurones. The presence of three shut states suggests that the M-channel openings appear in bursts. When bursts were determined as including the shortest shut state (τ_{s1}), they had short (τ_{b1}) and long (τ_{b2}) durations. Since τ_{b1} (11.0 ms) is equal to τ_{o1} (10.6 ms), the short bursts probably constitute short single channel openings which are adjacent to closings longer than τ_{s1} . At the same time, long bursts probably include both long and short channel openings.

There is some resemblance between these apparent burst durations and the kinetic components of the macroscopic M-current reported previously. Thus, τ_{b2} (80 ms at 30 mV depolarization) is not dissimilar to that for the macroscopic current relaxation originally reported in adult rat ganglion cells *in situ* using microelectrodes (about 70 ms at -30 mV; Constanti & Brown, 1981) and more recently in dissociated rat ganglion cells using nystatin-filled patch electrodes (88 ms; Selyanko *et al.* 1992) although other experiments on these cells with whole-cell patch electrodes (Owen *et al.* 1990) yielded a rather longer time constant of around 200 ms; noise spectra in both rat (Owen *et al.* 1990) and frog (Marrion *et al.* 1992) cells yielded two time constants roughly comparable to the time constants τ_{b1} and τ_{b2} recorded in the present experiments. The apparent correspondence between τ_{b2} and macroscopic current kinetics may, to some extent, be fortuitous, since (i) macroscopic current relaxations also suggest an additional, much slower component (Owen *et al.* 1990; Marrion *et al.* 1992), and (ii) in previous experiments on isolated patches from rat ganglion cells (which yielded not dissimilar sets of open and closed time distributions to those observed in the present experiments) no significant difference in single channel burst durations could be detected between individual patches showing 10-fold differences in the kinetics of the averaged currents (Stansfeld *et al.* 1993). In the latter study the kinetics of averaged currents was, instead, related to the channel substate behaviour: smaller conductance channels more readily gave a slower activation time course. By contrast, substate behaviour (transitions between different conductance levels) was rarely seen in cell-attached patches and neither activation kinetics recorded during voltage steps (Selyanko *et al.* 1992), nor channel kinetics under steady-state conditions (present results) seem to be dependent on the dominance of smaller or larger channels present in the patch.

Notwithstanding the apparent multiplicity of kinetic states suggested by the single channel records, the overall sensitivities of the open and shut states to changes in the membrane potential were consistent with the original kinetic model for $I_{K(M)}$ proposed by Adams *et al.* (1982a), i.e. depolarization increased the rates of channel opening (related to $1/\tau_{s1}$, $1/\tau_{s2}$, $1/\tau_{s3}$) and reduced the rates of channel closing (related to $1/\tau_{o1}$, $1/\tau_{o2}$). This was not an artifact of changes in channel current amplitude (and hence of short event detection) since (i) simulations suggested that such artifactual effects would be relatively small compared with recorded changes (Table 2), and (ii) the contribution of smaller conductance channels to the overall activity decreased, rather than increased, with depolarization. Furthermore, the slope factor for the voltage dependence of P_o (about 8 mV between 10 and 30 mV depolarization, Fig. 2B) accords with that for the macroscopic M-current originally recorded in rat ganglion cells (Constanti & Brown, 1981).

In contrast to the effect of potential changes, muscarine simply lengthened the

shut times without affecting open times. This also accords with the original observations on macroscopic currents in which muscarine did not alter the time course of the deactivation relaxations at hyperpolarized levels (Adams *et al.* 1982*b*; see also Owen *et al.* 1990). However, the lengthened shut times do imply that the time constant for the macroscopic relaxations might be lengthened at strongly depolarized levels (by about 50% at -30 mV) and the activation curve shifted toward more positive levels (by about 11 mV) in the presence of muscarine. This has not been previously noted, but such changes would be difficult to detect in macroscopic current recording because of the greatly reduced current amplitude and the difficulty in isolating $I_{K(M)}$ from other currents at ≤ -30 mV.

Finally, the difference between the effects of muscarine and membrane potential change on open-time distributions affords a convenient distinction which may be helpful in further studies aimed at determining the mechanism of M-channel closure by muscarinic agonists.

We thank Dr C. E. Stansfeld for her co-operation in these experiments, Dr A. J. Gibb for help with computation and simulation, and Ms Y. Vallis for tissue culture. This work was supported by the Wellcome Trust and the Medical Research Council. A. A. S. was in receipt of a Wellcome Trust Fellowship.

REFERENCES

- ADAMS, P. R., BROWN, D. A. & CONSTANTI, A. (1982*a*). M-currents and other potassium currents in bullfrog sympathetic neurones. *Journal of Physiology* **330**, 537–562.
- ADAMS, P. R., BROWN, D. A. & CONSTANTI, A. (1982*b*). Pharmacological inhibition of the M-current. *Journal of Physiology* **332**, 223–262.
- BROWN, D. A. (1983). Slow cholinergic excitation – a mechanism for increasing neuronal excitability. *Trends in Neurosciences* **6**, 302–307.
- BROWN, D. A. (1988*a*). M-currents. In *Ion Channels*, vol. 1, ed. NARAHASHI, T., pp. 55–94. Plenum Press, New York.
- BROWN, D. A. (1988*b*). M-currents: an update. *Trends in Neurosciences* **11**, 294–299.
- BROWN, D. A. & ADAMS, P. R. (1980). Muscarinic suppression of a novel voltage-sensitive K^+ current in a vertebrate neurone. *Nature* **283**, 673–676.
- BROWN, D. A., MARRION, N. V. & SMART, T. G. (1989). On the transduction mechanism for muscarine-induced inhibition of M-current in cultured rat sympathetic neurones. *Journal of Physiology* **413**, 469–488.
- COLQUHOUN, D. & SAKMANN, B. (1985). Fast events in single-channel currents activated by acetylcholine and its analogues at the frog muscle end-plate. *Journal of Physiology* **369**, 501–557.
- CONSTANTI, A. & BROWN, D. A. (1981). M-currents in voltage-clamped mammalian sympathetic neurones. *Neuroscience Letters* **24**, 289–294.
- LOPEZ, H. S. & ADAMS, P. R. (1989). A G protein mediates the inhibition of the voltage-dependent potassium M current by muscarine, LHRH, substance P and UTP in bullfrog sympathetic neurons. *European Journal of Neuroscience* **1**, 529–542.
- MARRION, N. V., ADAMS, P. R. & GRUNER, W. (1992). Multiple kinetic states underlying macroscopic M-currents in bullfrog sympathetic neurons. *Proceedings of the Royal Society B* **248**, 207–214.
- MARRION, N. V., SMART, T. G. & BROWN, D. A. (1987). Membrane currents in adult superior cervical ganglia in dissociated tissue culture. *Neuroscience Letters* **77**, 55–60.
- NEHER, E., MARTY, A., FUKUDA, K., KUBO, T. & NUMA, S. (1988). Intracellular calcium release mediated by two muscarinic receptor subtypes. *FEBS Letters* **240**, 88–94.
- OWEN, D. G., MARSH, S. J. & BROWN, D. A. (1990). M-current noise and putative M-channels in cultured rat sympathetic ganglion cells. *Journal of Physiology* **431**, 269–290.

- PENNEFATHER, P. (1986). The rate of activation of M-current at positive potentials in bullfrog sympathetic ganglion cells. *Biophysical Journal* **49**, 166a.
- PFAFFINGER, P. (1988). Muscarine and t-LHRH suppress M-current by activating an IAP-insensitive G-protein. *Journal of Neuroscience* **8**, 3343–3353.
- ROBBINS, J., TROUSLARD, J., MARSH, S. J. & BROWN, D. A. (1992). Kinetic and pharmacological properties of the M-current in rodent neuroblastoma × glioma hybrid cells. *Journal of Physiology* **451**, 159–185.
- SELYANKO, A. A., STANSFELD, C. E. & BROWN, D. A. (1992). Closure of potassium M-channels by muscarinic acetylcholine-receptor stimulants requires a diffusible messenger. *Proceedings of the Royal Society B* **250**, 119–125.
- STANSFELD, C. E., MARSH, S. J. & BROWN, D. A. (1990). Putative M-channels in cultured rat superior cervical ganglion (SCG) cells. *Journal of Physiology* **426**, 69P.
- STANSFELD, C. E., MARSH, S. J., GIBB, A. J. & BROWN, D. A. (1993). Identification of M-channels in outside-out patches excised from sympathetic ganglion cells. *Neuron* **10**, 639–654.